A NEW SPIN ON SPIN POLARIMETRY

Mark E. Pesses
Science Applications International Corporation
Spectropolarimetric Laboratory
4001 Fairfax Dr., Suite 800, Arlington, VA 22203
pessesm@saic.com

Eileen V. Ryan
New Mexico Institute Technology
Magdalena Ridge Observatory
801 Leroy Place, Socorro, NM 87801
eryan@admin.nmt.edu

ABSTRACT

Polarimetric observations of space objects can provide information on shape, surface roughness and electrical conductivity that are very difficult or impossible to obtain from non-polarimetric data. Nature does not give up this extra information freely, as polarimetric data acquisition is more complicated and cumbersome than acquisition of intensity-only data. Stokes' original paper reports that six separate observations are required to measure the four Stokes parameters. Researchers at AFRL/Kirtland recently showed that all four Stokes parameters can be measured via the Fourier analysis of the modulation of the intensity observed behind a rotating quarter-wave plate and a stationary linear polarizer. We present three new methods for measuring Stokes parameters that require a spinning polarizer and/or a spinning achromatic quarter-wave plate. Several applications of these new methods are discussed for obtaining spectropolarimetric data from space object-tracking telescopes.

1. BACKGROUND

Force Protection in Iraq and Afghanistan requires the ability to do stand-off threat detection in real-time. In response to this, Science Applications International Corporation (SAIC) developed techniques that can provide the warfighter with real-time capability to exploit Electro Optic (EO) polarimetric data. Hyperspectral imaging does not utilize the information contained in the look-angle dependence of reflected and emitted light. This information can be exploited to discriminate between objects based on: electrical conductivity; angularity; surface roughness / ground clumsiness, as well as, spectral and temperature signatures. Because of this, polarimetric data opens up the possibility of detecting things that might go undetected by other means. Polarimeters also are very good at detecting man-made objects. There are times when neither visible nor infrared light can do a good job of detecting an object that will stand out like a sore thumb when examined by a polarimeter.

Current real-time EO polarimetry sensors utilize the light intensity observed at two orthogonal positions of a linear polarization filter. This is currently done using a liquid crystal polarizer attached to a camera and synchronized to an internal timer. This method only allows the user to observe S1 or S2 but not both Stokes parameters at the same time. Hence the information contained in the Degree Of Linear Polarization (DOLP) and the Angle Of Polarization (AOP) are not observable. Furthermore, liquid crystal polarizers are not available at LWIR wavelengths. Also, the efficiency and response time of liquid crystal polarizers in extreme conditions of hot or cold have yet to been tested. In light of this, SAIC has investigated the feasibility of doing real-time EO polarimetry with conventional solid linear polarizer filters that continuously rotate.

The purpose of this paper is to described these methods and discuss their application to AMOS and AFRL targets of interest. Four "polarimetric" ground truth images of the ANDERR MAA Spacecraft taken at NRL in Feb 2005 and shown in Fig. 1. The images were taken with a SIGMA SD10 camera using an ASO setting of 800, a shutter speed of 1/15 s and an Aperture value of F4.5. The images were obtained using an Edmund Hoya LB-120 Daylight Blue color filter and an Edmund Techspec glass linear polarizer with an extinction ratio of 10,000: 1.

The orientation of the linear polarizer, going clockwise from the upper left, is 0 deg, 45 deg, 90 deg, and 135 deg, where 0 deg is horizontal and 90 deg vertical relative to the image.

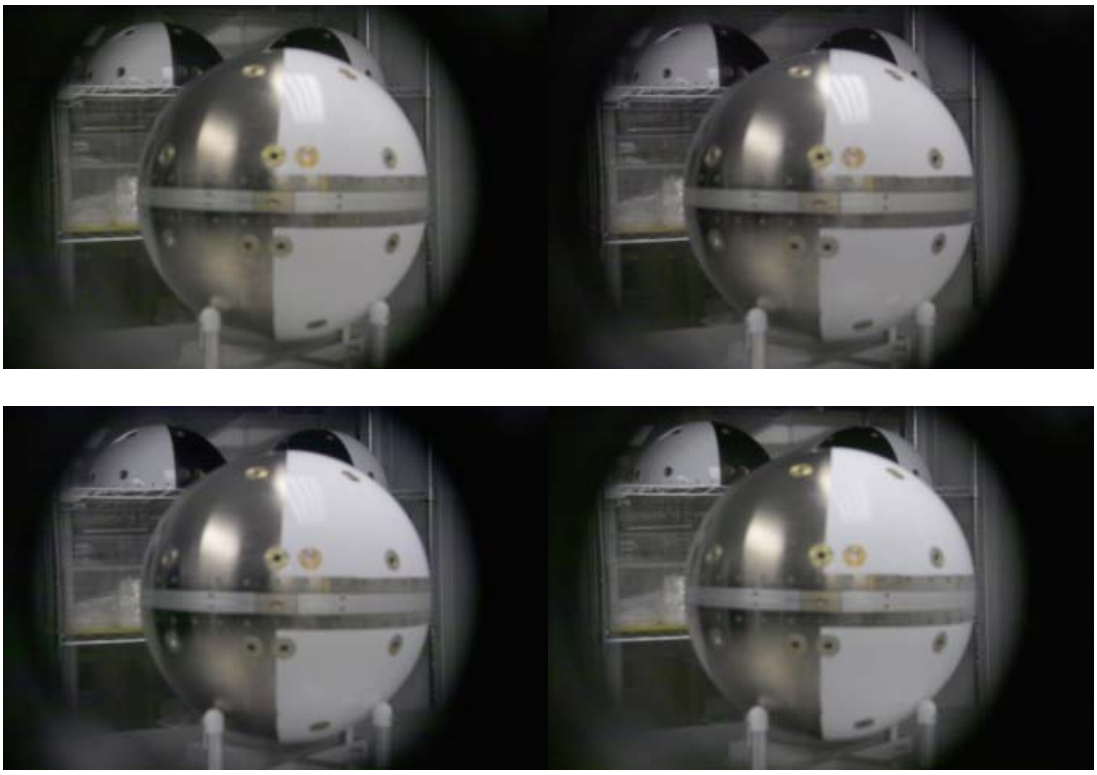

Fig. 1. Four "polarimetric" ground truth images of the ANDERR MAA Spacecraft The images were taken with a Daylight Blue color filter and a linear polarizer with an extinction ratio of 10,000: 1. The orientation of the linear polarizer, going clockwise from the upper left, is 0 deg, 45 deg, 90 deg, and 135 deg, where 0 deg is horizontal and 90 deg vertical relative to the image. False color images of S0, S1, S2, and AOP, calculated from the above images are shown in Fig. 2.

2. COORDINATE SYSTEM

The coordinate system for the spin polarimetry detector is shown in Fig. 2. The light source is at the far left. The positive Z-axis of the system is parallel to the propagation direction of the electromagnetic radiation being observed by the detector at the far right. The light first interacts with a quarter waveplate. The X-axis and Y-axis of the coordinate system are parallel with the quarter waveplate fast-axis and slow-axis, respectively. In between the quarter waveplate and the detector is a linear polarizer with the $\theta = 0^{O}$ polarizer angle parallel to the quarter waveplate fast-axis and the X-axis of the coordinate system.

3. POLARIZER INTENSITY EQUATION

The equation for how the intensity of light of wavelength λ varies by first passing through a waveplate that changes the phase between x and y components by α radians and then passing through an ideal linear polarizer is orientated and an angle θ to the x-axis is derived in [1] and is given by Eq. (1).

$$I_O(\lambda,\theta,\alpha,\varphi=0)=\frac{1}{2}\{S0(\lambda)+S1(\lambda)\mathrm{Cos}(2\theta)+[S2(\lambda)\mathrm{Cos}(\alpha)+S3(\lambda)\mathrm{Sin}(\alpha)]\mathrm{Sin}(2\theta)\} \quad (1)$$

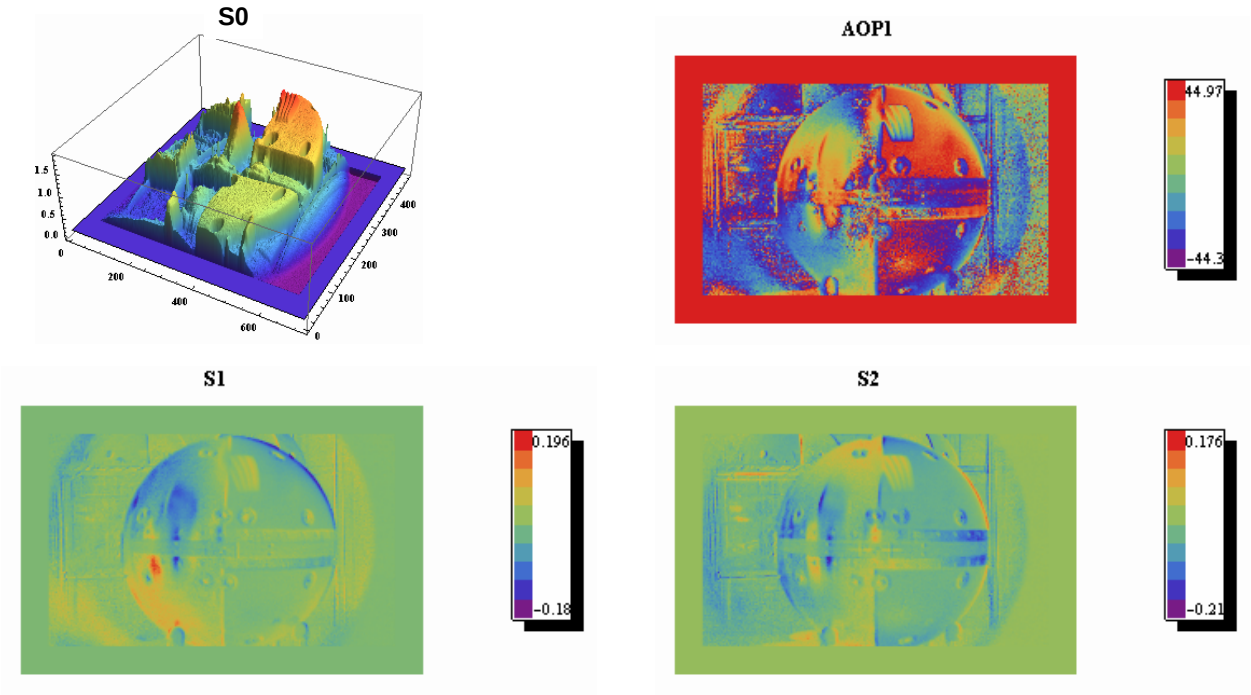

Figure 2. False color images of S0, S1, S2, and AOP calculated from the images shown in Fig. 1.

In the case where there is no retarding waveplate present ($\alpha = 0$) Eq. (1) reduces to

$$I_{LR}(\lambda,\theta) = \frac{1}{2}\left[S0(\lambda) + S1(\lambda)\,\mathrm{Cos}(2\theta) + S2(\lambda)\,\mathrm{Sin}(2\theta)\right] \tag{2}$$

In turn, Equation (2) can be expressed in terms of the Degree Of Linear Polarization (DOLP) and the Angle of Polarization (AOP), as shown in Eq.(3)

$$I_{LR}(\lambda,\theta) = \frac{S0(\lambda)}{2}\left\{1 + DOLP(\lambda)\,\mathrm{Cos}\left[2\left(AOP(\lambda) - \theta\right)\right]\right\} \tag{3}$$

where the expressions $DOLP = \dfrac{\sqrt{S1^2 + S2^2}}{S0}$ and $AOP = -\dfrac{1}{2}\,\mathrm{ArcTan}\left(\dfrac{S2}{S1}\right)$ have been used and the λ dependence has been suppressed. Equation (3) shows the DOLP has the same form as a first order anisotropy amplitude.

Equation (3) can be used to give another definition for DOLP and SO

$$DOLP = \frac{I_{LR}(\max) - I_{LR}(\min)}{I_{LR}(\max) + I_{LR}(\min)} \tag{4}$$

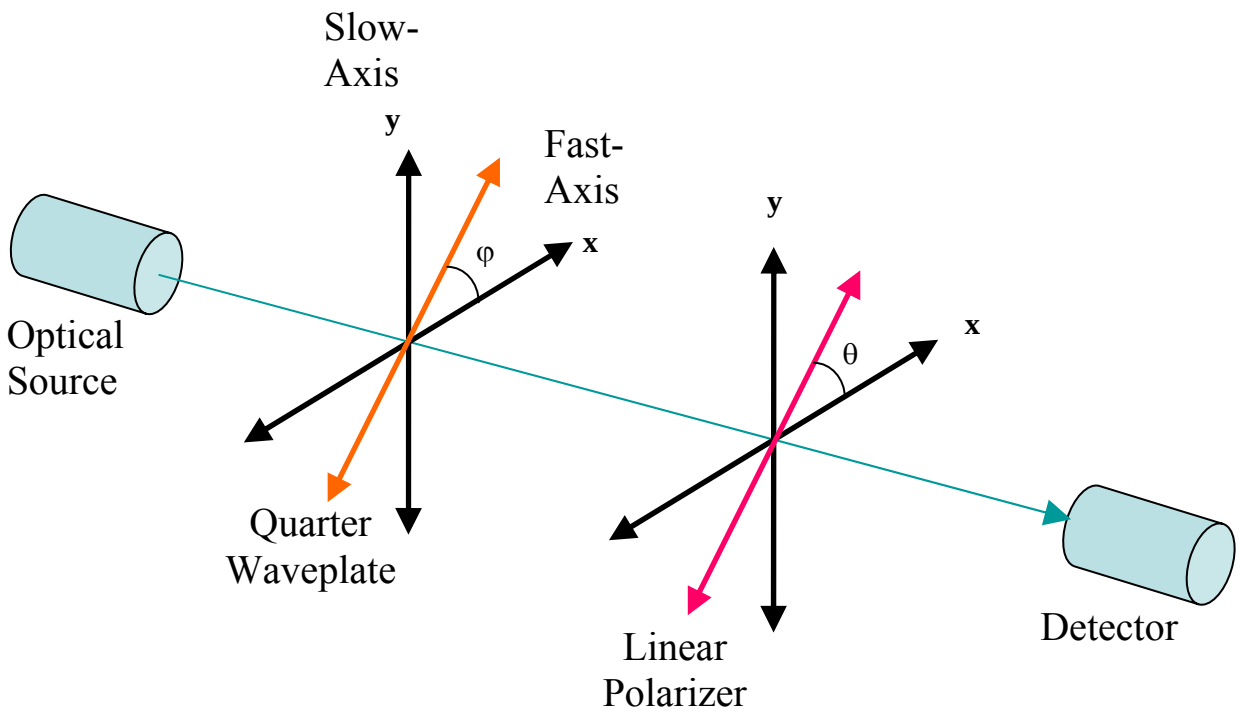

Figure 3. The polarimetric detector coordinate system used in this paper.

Here max and min refer to the maximum and minimum value of the observed intensity as the linear polarizer angle varies. In the case where there is a retarding waveplate present with $\alpha = \pi/2$ and $\varphi=0$ Eq. (1) reduces to

$$I_O(\lambda,\theta,\alpha=\pi/2,\varphi=0)=\frac{1}{2}\{S0(\lambda)+S1(\lambda)\mathrm{Cos}(2\theta)+S3(\lambda)\mathrm{Sin}(2\theta)\} \quad (5)$$

and where there is a retarding waveplate present with $\alpha = \pi/2$ and φ is a variable Eq. (1) reduces to

$$I_{QWR}(\lambda,\theta=0,\alpha=\pi/2,\varphi)=\frac{1}{2}\left\{S0(\lambda)+\frac{1}{2}[S1(\lambda)+S1(\lambda)\mathrm{Cos}(4\varphi)+S2(\lambda)\mathrm{Sin}(4\varphi)]+S3(\lambda)\mathrm{Sin}(2\varphi)\right\} \quad (6)$$

4. SPIN POLARIMETRY

Traditionally, four independent measurements are needed to determine the first three Stokes parameters S0, S1, S2, and two additional independent measurements are required to obtain the value of the Stokes parameters S3. A simplification to this process has been proposed by Refs [2], [3], [4], [5], and [6], via evaluating the Stokes parameters in Eq (6) by doing a truncated Fourier series analysis of the equation. The results are given below, with the wavelength dependence suppressed.

$$\begin{aligned} S0 &= A - C \\ S1 &= 2C \\ S2 &= 2D \\ S3 &= B \end{aligned} \tag{7}$$

Where,

$$A = \frac{1}{\pi}\int_0^{2\pi} I_O(\varphi)\,d\varphi \quad B = \frac{2}{\pi}\int_0^{2\pi} I_O(\varphi)\,\mathrm{Sin}2\varphi\,d\varphi \quad C = \frac{2}{\pi}\int_0^{2\pi} I_O(\varphi)\,\mathrm{Cos}4\varphi\,d\varphi$$

$$D = \frac{2}{\pi}\int_0^{2\pi} I_O(\varphi)\,\mathrm{Sin}4\varphi\,d\varphi$$

A new "spin" method for calculating the Stokes parameter using Eq. (6) is given below.

$$\begin{aligned} S0 &= A + B \\ DOCP &= (A - B)/SO \\ DOLP^2 &= \frac{32 * D}{SO^2} - 4 * DOCP^2 \\ AOP &= \frac{1}{2} * \mathrm{ArcCos}\left(\frac{4 * C - 2 * S0}{DOLP}\right) \end{aligned} \tag{8}$$

Where,

$$A = I_O(0, \pi/4, \pi/2) \quad B = I_O(0, 3\pi/4, \pi/2) \quad C = \frac{1}{\pi}\int_{\varsigma}^{\varsigma+\pi} I_O(0, \varphi, \pi/2)\,d\varphi \tag{9}$$

$$D = \frac{1}{\pi}\int_{\varsigma}^{\varsigma+\pi} I_O^2(0, \varphi, \pi/2)\,d\varphi - C^2$$

And ζ is an arbitrary angle.

Another new "spin" method for calculating the Stokes parameter utilizes the mean and variances of Eq. (5) and Eq. (6). The "spin average" value of the intensity in Eq. (5), i.e. the value of the intensity averaged over all the full range of linear polarizer filter angles of $0 \le \theta < n\pi$ is,

$$\langle I_{LR}(\lambda, \theta)\rangle = \langle I_O(\lambda, \theta, \alpha)\rangle = \frac{\int_{\varsigma}^{\varsigma+n\pi} I_O(\lambda, \theta, \alpha)\,d\theta}{n\pi} = \frac{S0(\lambda)}{2} \tag{10}$$

where ζ is an arbitrary angle and n is a real integer not equal to zero. Equation (6) shows that the "spin average" value of the intensity is independent of the amount of polarization present and the value of the phase retardance being used.

The "spin average" value of the intensity in Eq. (6), i.e. the value of the intensity averaged over all the full range of quarter wave plate angles of $0 \leq \varphi < n\pi$ is,

$$\left\langle I_{QWR}(\lambda,\varphi)\right\rangle = \frac{\int_{\zeta}^{\zeta+n\pi} I_{QWR}(\lambda,\varphi)d\varphi}{n\pi} = \frac{S0(\lambda)}{2} + \frac{S1(\lambda)}{4} \tag{11}$$

The "spin variance" value of the intensity in Eq. (5), $\sigma\left[I_{LR}(\lambda,\theta)\right] = \left\langle I_{LR}^2(\lambda,\theta)\right\rangle - \left\langle I_{LR}(\lambda,\theta)\right\rangle^2$

is given by Eq. (12)

$$\frac{\int_{\zeta}^{\zeta+n\pi} I_{LR}^2(\lambda,\theta)d\theta}{n\pi} - \left\langle I_{LR}(\lambda,\theta)\right\rangle^2 = \frac{S1^2(\lambda)}{8} + \frac{S2^2(\lambda)}{8} \tag{12}$$

And the "spin variance" value of the intensity in Eq. (6), $\sigma\left[I_{QWR}(\lambda,\varphi)\right] = \left\langle I_{QWR}^2(\lambda,\varphi)\right\rangle - \left\langle I_{QWR}(\lambda,\varphi)\right\rangle^2$

is given by Eq. (13)

$$\frac{\int_{\zeta}^{\zeta+n\pi} I_{QWR}^2(\lambda,\varphi)d\varphi}{n\pi} - \left\langle I_{QWR}(\lambda,\varphi)\right\rangle^2 = \frac{S1^2(\lambda)}{32} + \frac{S2^2(\lambda)}{32} + \frac{S3^2(\lambda)}{8} \tag{13}$$

Simultaneously solving Eqs. (10-13) for the four Stokes Parameters gives:

$$\begin{aligned} S0(\lambda) &= 2*\left\langle I_{LR}(\lambda,\theta,\alpha)\right\rangle \\ S1(\lambda) &= 4*\left\langle I_{QWR}(\lambda,\theta)\right\rangle - 2*S0(\lambda) \\ S2(\lambda)^2 &= 8*\sigma\left[I_{LR}(\lambda,\theta)\right] - S1(\lambda)^2 \\ S3(\lambda)^2 &= 8*\sigma\left[I_{QWR}(\lambda,\varphi)\right] - 2*\sigma\left[I_{LR}(\lambda,\theta)\right] \end{aligned} \tag{14}$$

5. EFFECTS OF SPIN BLURRING

Implementing the new methods for getting the full Stokes parameters requires discretely evaluating the spin average and spin variance of the intensity. Assume that the intensity is measured over n internals given by
$\varphi_n - \delta/2 < \varphi < \varphi_n - \delta/2$

$$\int_{\theta_n-\delta/2}^{\theta_n+\delta/2} I_O(\varphi)/\delta = \frac{1}{2}\left\{S0 + \frac{1}{2}\left[S1 + S1\mathrm{Cos}\left(4\theta_n\right) + S2\ \mathrm{Sin}\left(4\theta_n\right)\right]\frac{\mathrm{Sin}(2\delta)}{2\delta} + S3\mathrm{Sin}\left(2\theta_n\right)\frac{\mathrm{Sin}(\delta)}{\delta}\right\} \quad (15)$$

The $\mathrm{Sin}(\delta)/\delta$ and $\mathrm{Sin}(2\delta)/2\delta$ terms result from going from a continuous to a discrete evaluation of means and variances.

$$S0_R = 2\mu_{LO} \quad S1_R = 4\mu_{QO} - 2S0_R \quad S2_R^2 = 8\frac{\delta^2}{\mathrm{Sin}^2(\delta)}\sigma_{LO} - S1_R^2$$

$$S3_R^2 = 8\frac{\delta^2}{\mathrm{Sin}^2(\delta)}\sigma_{QO} - \frac{S1_R^2 + S2_R^2}{64} * \frac{\mathrm{Sin}^2(2\delta)}{\mathrm{Sin}^2(\delta)} \quad (16)$$

Where the subscripts "R" and "O" refer to real and observed values of the spin-means, μ, and spin-variances, σ.

6. ASTEROID AND COMET POLARIMETRIC STUDIES

Asteroids and other small bodies in the solar system are illuminated by reflected sunlight as they rotate in the course of their orbit around the Sun. Characterizing the polarization state of this light can reveal important insights about the surface properties of these bodies. Specifically, the state of linear polarization of light scattered by an irregular surface is indicative of the microstructure of the surface and its relative composition. As the asteroid revolves around the Sun, its illumination geometry will vary (i.e., the phase angle relative to observers on the Earth changes). Measuring the variation in the degree of linear polarization as a function of phase angle can yield valuable information, including inferences about the geometric albedo of the asteroid. This parameter, when coupled with the visible brightness of the object, can then be used to infer the asteroid's size. For objects on a potential collision course with the Earth, data of this nature can be especially important to obtain as it gives a measure of the scale of the threat. The albedo is also important for classifying the object's material composition, also a factor in hazard mitigation.

One of the most unique contributions to asteroid and comet characterization that polarization studies can provide is actual data on the surface texture of the regolith covering these bodies. Spacecraft data (e.g., [7]) has confirmed the existence of thick regolith layers on asteroidal surfaces created by the consistent and repeated bombardment of impacting bodies over the course of the solar system's history. Understanding the particle size distributions and how they vary from object to object relative to distance from the Sun and degree of volatility (i.e., comets versus asteroids) would enhance our understanding of how primitive bodies form and dynamically evolve.

A ground-based observational campaign guided by the polarimetric techniques discussed in this paper would focus on two main objectives:

- Determining reliable diameters (to augment radiometric data) for asteroids in the main belt as well as in the near-Earth zone by acquiring estimates of their albedos.

- Studying the surface property differences between asteroids and comets, and objects in the transition zone (i.e., comets that have lost most of their volatiles).

This program of ground-based observations would be accomplished using the Magdalena Ridge 2.4-meter Telescope Facility located at 10,612 feet in the mountains of central New Mexico. The site has excellent seeing profiles, and the telescope is newly commissioned and state-of the-art including easy remote accessibility,

streamlined scheduling, and computer control of all support systems. Using polarimetric techniques to investigate light scattering effects on small bodies, including shadowing and coherent backscattering, should enhance existing polarization databases as well as provide new and unique results.

7. Conclusions

Three new spin polarimetry methods for determining the value of the Stokes parameters have been presented. The next steps are to test them for accuracy, robustness, hardware implimentbility and ease of integration with existing sensor systems.

8. References

1. Born, M. and E. Wolf, *Principles of Optics*, Cambridge University Press, New York, NY, 1980.

2. Aspnes, D. E., Fourier Transform Detection System for Rotating-Analyzer Ellipsometers, Opt*. Commun.*, **8**, p. 222, 1973.

3. Collette, E. ed., *Polarized Light: Fundamentals and Applications,* Marcel Dekker Inc., p. 103. New York, 1993.

4. Williams. P. A., Rotating-wave-plate Stokes polarimeter for differential group delay measurements of polarization-mode dispersion, *Applied Optics*, **38**, No. 31, p. 6508, 1 November 1999.

5. Chennault, D. B., Duggin, M. J., Egan, W. G., Goldstein, D. K., eds, *Polarization Analysis, Measurement, and Remote Sensing III*, Proceedings of SPIE, **4133,** 2000.

6. Collett, E., *Field Guide to Polarization*, SPIE Press, Bellingham, WA, 2005.

7. Chapman, C. R., Cratering on asteroids from Galileo and NEAR–Shoemaker, Bottke, W. F., Cellino, A., Paolicchi, P., and R.P. Binzel, eds, *Asteroids III*, Univ. of Arizona Press, Tucson, p. 315, 2002.